

Nano Research

October 2020

Volume 13 · Number 10



Q K 2 0 4 0 1 6 1

Nanomaterials for radiotherapeutics-based multimodal synergistic cancer therapy

Nanotechnologies for enhancing cancer immunotherapy

Advances of biological-camouflaged nanoparticles delivery system



TSINGHUA
UNIVERSITY PRESS



Springer



Project for Enhancing International
Impact of China STM Journals

Contents

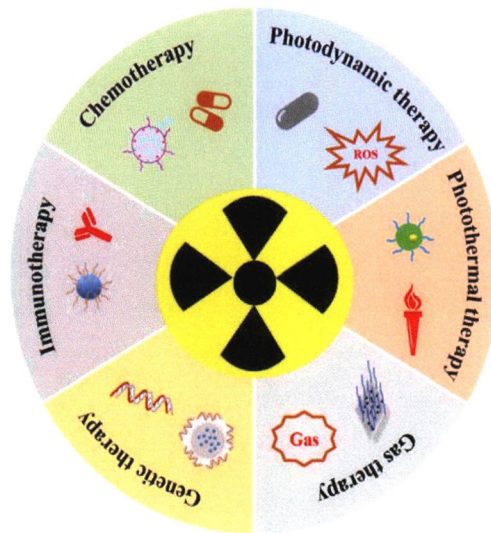
Review Articles

Nanomaterials for radiotherapeutics-based multimodal synergistic cancer therapy

Xi Yang¹, Ling Gao¹, Qing Guo², Yongjiang Li¹, Yue Ma¹, Ju Yang¹, Changyang Gong^{1,*}, and Cheng Yi^{1,*}

¹ Sichuan University, China

² Taizhou People's Hospital, China



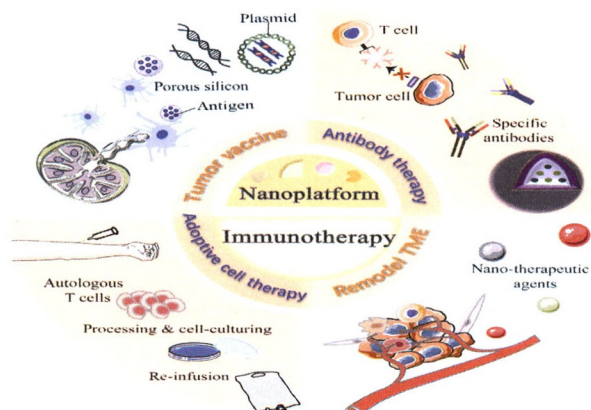
In this review, we discuss opportunities for a synergistic cancer therapy by combining radiotherapy based on nanomaterials designed for chemotherapy, photodynamic therapy, photothermal therapy, gas therapy, genetic therapy, and immunotherapy.

2579–2594

Nanotechnologies for enhancing cancer immunotherapy

Jingxian Yang, Chunhui Wang, Shuo Shi*, and Chunyan Dong*

Tongji University, China



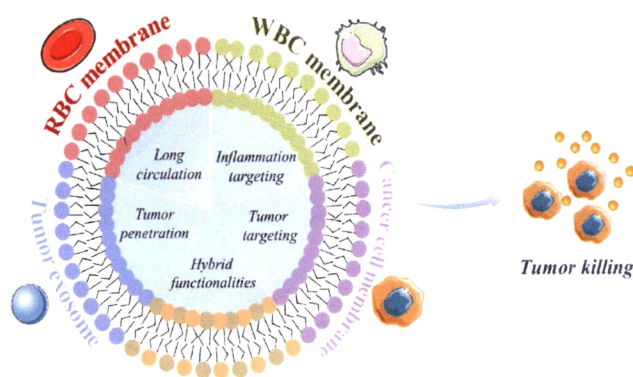
Based on the medical introduction of cancer immunotherapy and the application of nanomaterial delivery system in tumor treatments, this review summarizes the recent advances in nanoparticle-based technology combined with the hot spots in the field of immunotherapy. The aim is to develop better immunotherapy nano-tools for clinical use under the guidance of existing research results.

2595–2616

Advances of biological-camouflaged nanoparticles delivery system

Yanlin Chen and Kui Cheng*

Southern Medical University, China



Different cell membrane-coated nanoparticles are used for tumor therapy.

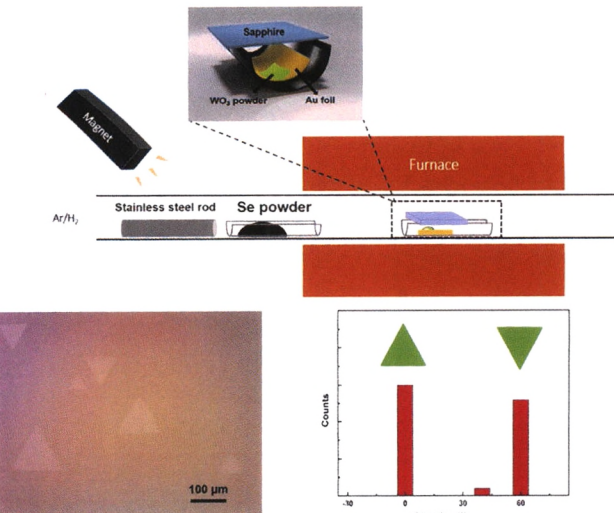
2617–2624

Research Articles

Gold-vapor-assisted chemical vapor deposition of aligned monolayer WSe₂ with large domain size and fast growth rate

Mingrui Chen, Anyi Zhang, Yihang Liu, Dingzhou Cui, Zhen Li, Yu-Han Chung, Sai Praneetha Mutyala, Matthew Mecklenburg, Xiao Nie, Chi Xu, Fanqi Wu, Qingzhou Liu, and Chongwu Zhou*

University of Southern California, Los Angeles, USA



Gold vapor was introduced into the chemical vapor deposition (CVD) process as a catalyst to assist the growth of WSe₂. Highly aligned monolayer WSe₂ triangular flakes with large domain size ($130 \mu\text{m}$) and fast growth rate ($4.3 \mu\text{m}\cdot\text{s}^{-1}$), and continuous monolayer films with good uniformity were achieved.

2625–2631

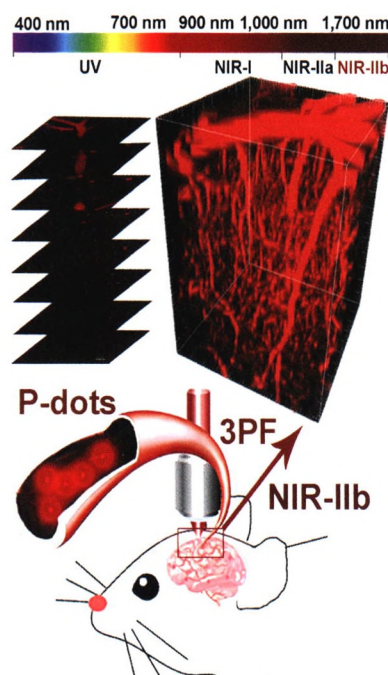
NIR-IIb excitable bright polymer dots with deep-red emission for *in vivo* through-skull three-photon fluorescence bioimaging

Nuernisha Alifu^{1,2}, Abudureheman Zebibula², Hequn Zhang², Huawei Ni², Liang Zhu², Wang Xi^{2,*}, Yalun Wang², Xueliang Zhang^{1,*}, Changfeng Wu³, and Jun Qian^{2,*}

¹ Xinjiang Medical University, China

² Zhejiang University, China

³ South University of Science and Technology, China



The near-infrared IIb (NIR-IIb) excitable deep-red emissive semiconducting polymer dots (P-dots) with bright three-photon fluorescence (3PF) under 1,550 nm femtosecond laser excitation were prepared and functionalized. Then the P-dots were utilized for *in vivo* 3PF cerebral vasculature microscopic imaging of mice with and without the brain skull.

2632–2640

Unexpected Kirkendall effect in twinned icosahedral nanocrystals driven by strain gradient

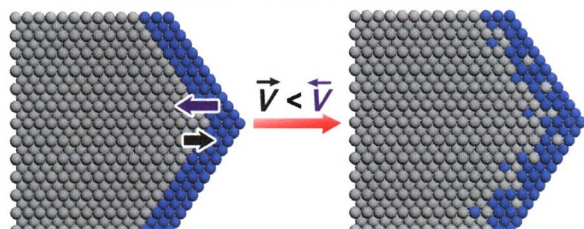
Jingbo Huang¹, Yucong Yan^{1,2}, Xiao Li¹, Xurong Qiao³, Xingqiao Wu¹, Junjie Li¹, Rong Shen¹, Deren Yang^{1,*}, and Hui Zhang^{1,*}

¹ Zhejiang University, China

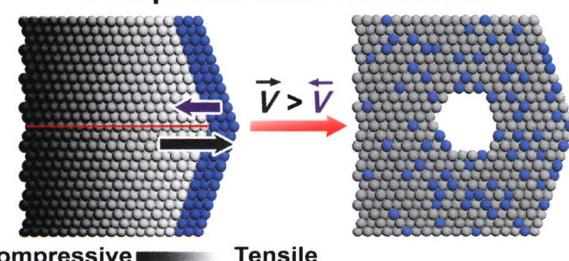
² SAIC Motor Corporation Limited, China

³ China University of Petroleum, China

Traditional Kirkendall effect



Unexpected Kirkendall effect



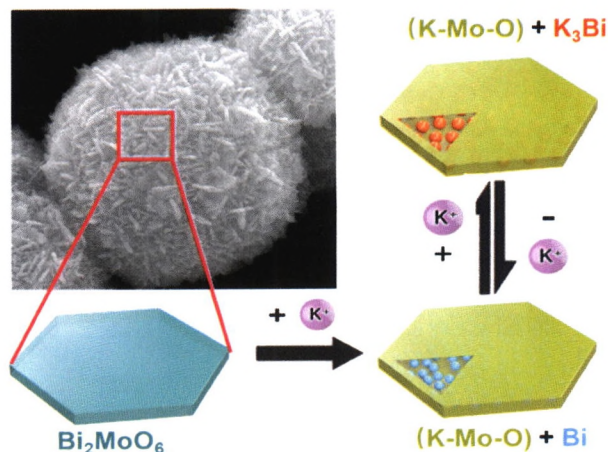
Kirkendall effect unexpectedly takes place when diffusing intrinsically faster Cu atoms into Pd icosahedra. The strain gradient arising from the multiple twins of the icosahedra is the key to drive such Kirkendall effect, leading to the formation of hollow structures.

2641–2649

Unveiling nanoplates-assembled Bi_2MoO_6 microsphere as a novel anode material for high performance potassium-ion batteries

Junxian Hu, Yangyang Xie, Jingqiang Zheng, Yanqing Lai, and Zhian Zhang*

Central South University, China



Bi_2MoO_6 microsphere assembled by two-dimensional (2D) nanoplate exhibits good potassium storage performance and performs a combination mechanism of conversion reaction and alloying/dealloying reaction.

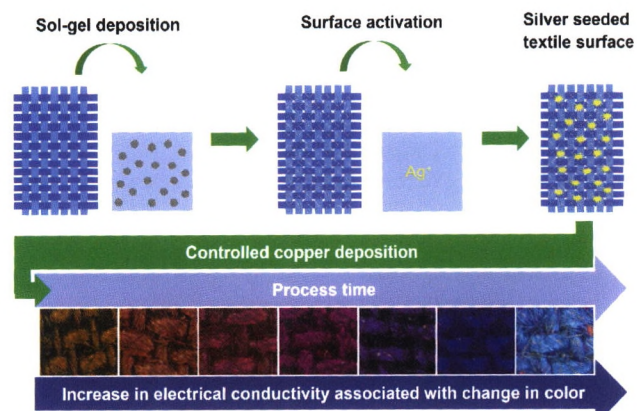
2650–2657

Tunable colors and conductivity by electroless growth of $\text{Cu}/\text{Cu}_2\text{O}$ particles on sol-gel modified cellulose

Justus Landsiedel^{1,*}, Waleri Root¹, Christian Schramm¹, Alexander Menzel¹, Steffen Witzleben², Thomas Bechtold¹, and Tung Pham^{1,*}

¹ University of Innsbruck, Austria

² Bonn-Rhein-Sieg University of Applied Sciences, Germany



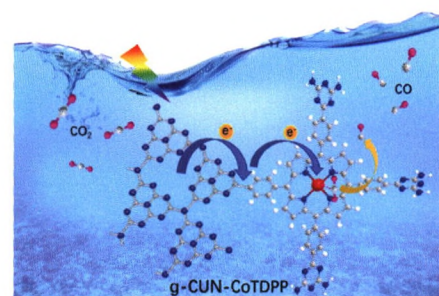
In situ growth and immobilization of copper nanoparticles on cellulose textiles results in tunable coloration and electrical conductivities.

2658–2664

An efficient visible-light photocatalyst for CO₂ reduction fabricated by cobalt porphyrin and graphitic carbon nitride via covalent bonding

Shufang Tian, Sudi Chen, Xitong Ren, Yaoqing Hu, Haiyan Hu, and Jiajie Sun*, and Feng Bai*

Henan University, China



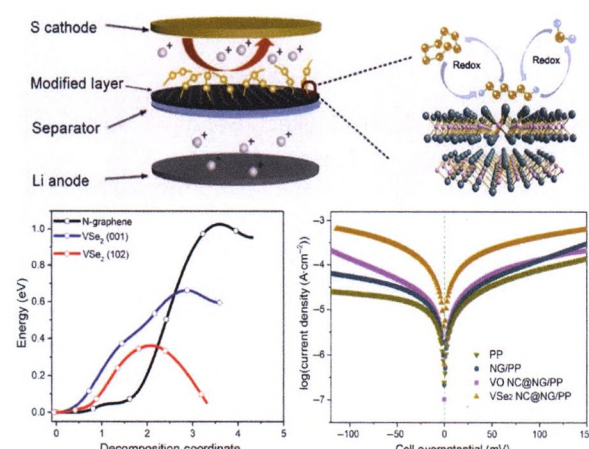
The functional integrated visible light photocatalyst for CO₂ reduction was prepared by combining homogeneous catalyst metalloporphyrin CoTDPP with the heterogeneous photosensitizer graphitic carbon nitride via covalent bonding. The strong interaction between catalyst unit and photosensitizer unit is conducive to the separation and migration of photogenerated charge carriers and the metalloporphyrin CoTDPP not only provides single site catalytic center but also effectively broadens the visible light absorption range of the functional integrated photocatalyst. The g-C3N4-CoTDPP exhibited excellent photocatalytic performance for CO₂ reduction with CO as the major product at an average evolution rate of 57 μmol/(g·h) and the selectivity of 79% over competing H₂ evolution.

2665–2672

Bonding VSe₂ ultrafine nanocrystals on graphene toward advanced lithium-sulfur batteries

Wenzhi Tian, Baojuan Xi, Yu Gu, Qiang Fu, Zhenyu Feng, Jinkui Feng, and Shenglin Xiong*

Shandong University, China



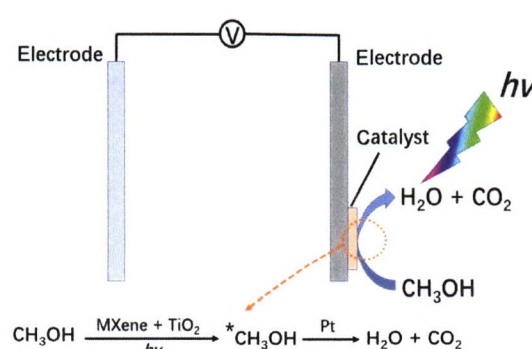
VSe₂ ultrafine nanocrystals immobilized on the nitrogen-doped graphene hybrid nanosheets (VSe₂ NC@NG) as a new polysulfides barrier are synthesized via a self-template strategy, which possess more exposed sulfophilic planes of VSe₂, as well as benefit the uniform nucleation of Li₂S—making this system an excellent polysulfides barrier for lithium–sulfur batteries.

2673–2682

A photoactive process cascaded electrocatalysis for enhanced methanol oxidation over Pt-MXene-TiO₂ composite

Yue Sun, Yunjie Zhou, Yan Liu, Qingyao Wu, Mengmeng Zhu, Hui Huang, Yang Liu*, Mingwang Shao*, and Zhenhui Kang*

Soochow University, China



A Pt-MXene-TiO₂ composite exhibits highly efficient methanol oxidation reaction (MOR) performance with light irradiation via a photo-active cascaded electro-catalytic process.

2683–2690

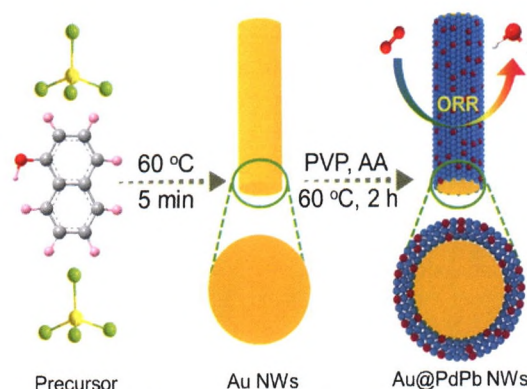
Trimetallic Au@PdPb nanowires for oxygen reduction reaction

Xian Jiang^{1,2,3}, Yuxin Xiong³, Ruopeng Zhao², Jiancheng Zhou^{1,*}, Jong-Min Lee^{2,*}, and Yawen Tang^{3,*}

¹ Southeast University, China

² Nanyang Technological University, Singapore

³ Nanjing Normal University, China



Trimetallic Au@PdPb nanowires (NWs) are synthesized by using pre-fabricated ultrathin Au nanowires as the one-dimensional template. The Au@PdPb NWs are demonstrated to be active and stable for the oxygen reduction reaction (ORR), much better than those of commercial Pd black and bimetallic Au@Pd NWs. Considering facile synthesis method and excellent ORR performance, the developed Au@PdPb NWs may have great potential in the field of fuel cells.

2691–2696

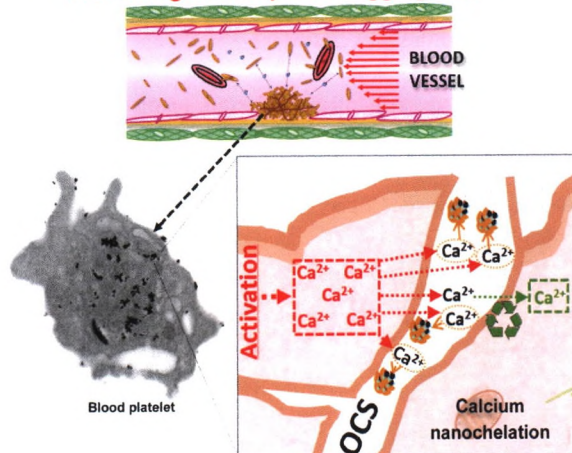
Controlling human platelet activation with calcium-binding nanoparticles

David Cabrera¹, Karen Walker¹, Sandhya Moise^{1,2}, Neil D. Telling¹, and Alan G. S. Harper^{1,*}

¹ Keele University, UK

² University of Bath, UK

Preventing human platelet aggregation



Calcium-binding magnetic nanoparticles are an effective anti-platelet nanomedicine. These nanoparticles function by chelating calcium in the open canalicular system (OCS; a space formed by the infolding of the platelet plasma membrane) interfering with normal Ca²⁺ signaling pathways that drive platelet aggregation.

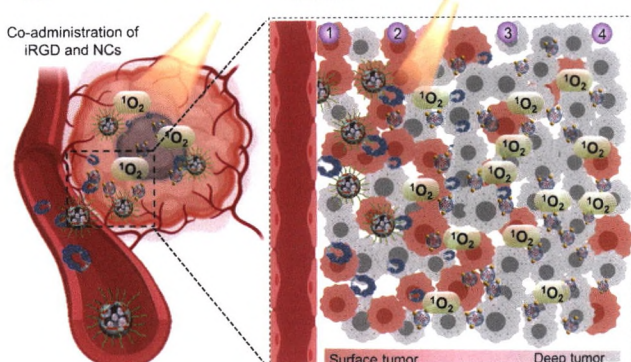
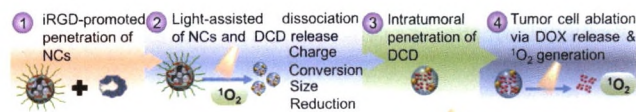
2697–2705

iRGD-reinforced, photo-transformable nanoclusters toward cooperative enhancement of intratumoral penetration and antitumor efficacy

Jing Yan¹, Rongying Zhu², Fan Wu¹, Ziyin Zhao¹, Huan Ye¹, Mengying Hou¹, Yong Liu^{1,*}, and Lichen Yin^{1,*}

¹ Soochow University, China

² The Second Affiliated Hospital of Soochow University, China



iRGD-assisted and photo-transformable nanoclusters mediate cooperative enhancement of intratumoral penetration and programmed tumor ablation.

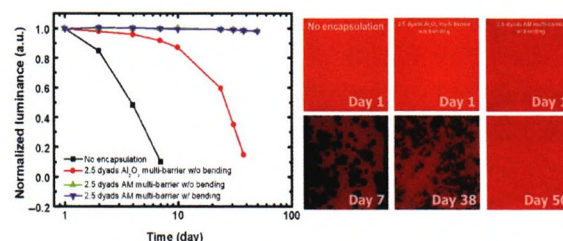
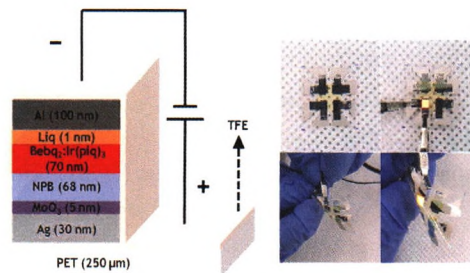
2706–2715

Reliable high temperature, high humidity flexible thin film encapsulation using $\text{Al}_2\text{O}_3/\text{MgO}$ nanolaminates for flexible OLEDs

Ki Suk Kang¹, So Yeong Jeong¹, Eun Gyo Jeong^{2,*}, and Kyung Cheol Choi^{1,*}

¹ Korea Advanced Institute of Science and Technology (KAIST), Republic of Korea

² Chonnam National University, Republic of Korea



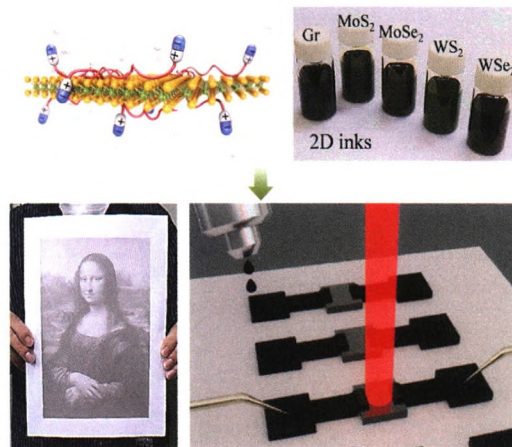
An $\text{Al}_2\text{O}_3/\text{MgO}$ nanolaminate was fabricated and it exhibited greatly improved hydrolysis resistance in harsh environmental conditions than Al_2O_3 . An actual encapsulated operating device was tested under bending stress and the device demonstrated excellently stable shelf-lifetime in a harsh environment.

2716–2725

Zwitterion-assisted transition metal dichalcogenide nanosheets for scalable and biocompatible inkjet printing

Hyekjung Lee, Min Koo, Chanho Park, Madhumita Patel, Hyowon Han, Tae Hyun Park, Pawan Kumar, Won-Gun Koh, and Cheolmin Park*

Yonsei University, Republic of Korea



Various two-dimensional transition metal dichalcogenide (TMD) nanosheets, in addition to few-layered graphene, are inkjet-printed using a novel liquid-phase exfoliation process based on zwitterionic dispersants in water. Aqueous, biocompatible zwitterionic inks with TMD nanosheets are suitable for conventional office inkjet printing, giving rise to the mechanically flexible, printed arrays of two-terminal, parallel type photodetectors with pixelated TMD channels.

2726–2734

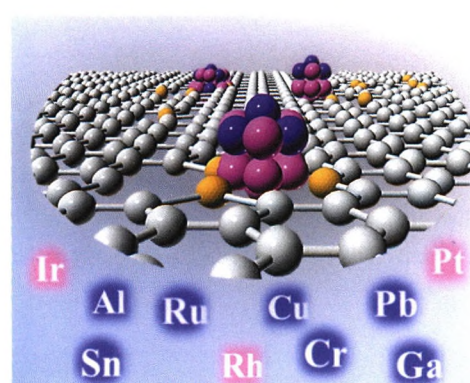
A library of carbon-supported ultrasmall bimetallic nanoparticles

Shi-Long Xu¹, Shan-Cheng Shen¹, Ze-Yue Wei¹, Shuai Zhao¹, Lu-Jie Zuo¹, Ming-Xi Chen¹, Lei Wang¹, Yan-Wei Ding¹, Ping Chen², Sheng-Qi Chu³, Yue Lin^{1,*}, Kun Qian^{1,*}, and Hai-Wei Liang^{1,*}

¹ University of Science and Technology of China, China

² Anhui University, China

³ Institute of High Energy Physics, Chinese Academy of Sciences, China



A library of ultrasmall bimetallic nanoparticles with average particle sizes ranging from 0.7 to 1.4 nm are prepared on mesoporous sulfur-doped carbon supports. The synthetic approach is based on the strong chemical interaction between the doped sulfur atoms on carbons and metals, which suppresses the metal aggregation during H₂-reduction and ensures the formation of small-sized and alloyed bimetallic nanoparticles.

2735–2740

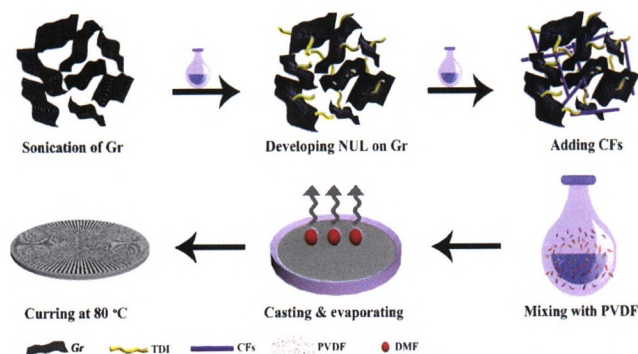
Enhancing through-plane thermal conductivity of fluoropolymer composite by developing *in situ* nano-urethane linkage at graphene–graphene interface

Muhammad Maqbool¹, Haichang Guo¹, Akbar Bashir¹, Ali Usman¹, Adeel Y. Abid¹, Guansong He², Yanjuan Ren¹, Zeeshan Ali^{1,3}, and Shulin Bai^{1,*}

¹ Peking University, China

² Institute of Chemical Materials, Chinese Academy of Engineering Physics (CAEP), China

³ National University of Sciences and Technology (NUST), Pakistan



The nanourethane linkage (NUL) based graphene (Gr) and carbon fibers (CFs) 3D architecture (NUL-Gr/CFs) is fabricated, which is further employed in making composite of polyvinylidene fluoride (PVDF). Herein, toluene diisocyanate (TDI) is utilized to develop NUL.

2741–2748

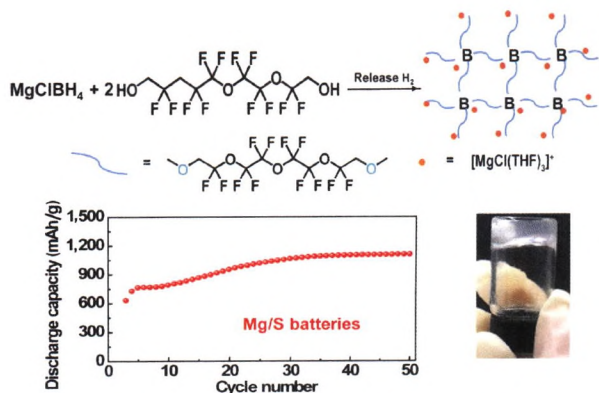
A non-nucleophilic gel polymer magnesium electrolyte compatible with sulfur cathode

Haiyan Fan^{1,2}, Yuxing Zhao³, Jianhua Xiao³, Jifang Zhang³, Min Wang^{1,2}, and Yuegang Zhang^{2,3,*}

¹ University of Science and Technology of China, China

² Suzhou Institute of Nano-Tech and Nano-Bionics, Chinese Academy of Sciences, China

³ Tsinghua University, China



Gel-type electrolytes are advantageous in terms of safety and flexibility compared with liquid electrolytes. Here, a non-nucleophilic gel-type magnesium chloride-(fluorinated tetraethylene glycolic)borate (MgCl-FTGB) electrolyte is synthesized. Mg deposition and stripping can be conducted with high rate and low overpotential in this electrolyte. It is also compatible with S cathode and enables stable cycling of Mg/S batteries.

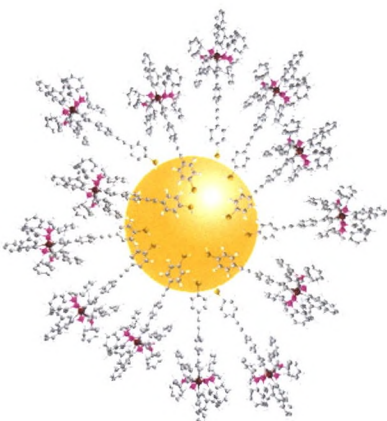
2749–2754

Hybrids of gold nanoparticles and oligo(p-phenyleneethynylene)s end-functionalized with alkynylruthenium groups: Outstanding two-photon absorption in the second biological window

Cristóbal Quintana¹, Mahbod Morshedi¹, Jun Du¹, Joseph P. L. Morrall¹, Jan K. Zarba², Marek Samoc², Marie P. Cifuentes¹, and Mark G. Humphrey^{1,*}

¹ Australian National University, Australia

² Wroclaw University of Science and Technology, Poland



Oligo(p-phenyleneethynylene)s (OPEs) end-capped with (alkynyl)bis(diphosphine)ruthenium and thiol/thiolate groups stabilize ca. 2 nm diameter gold nanoparticles (AuNPs) affording OPE/AuNP hybrids that display long-term stability in solution (more than a month), good solubility in organic solvents, reversible ruthenium-centered oxidation, and transparency beyond 800 nm, and possess very strong nonlinear absorption activity at the first biological window, and unprecedented two-photon absorption activity in the second biological window (σ_2 up to 38,000 GM at 1,050 nm).

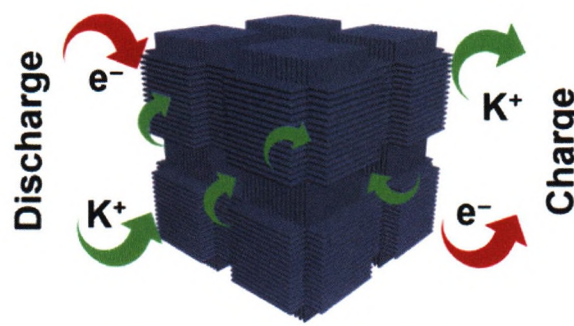
2755–2762

Edge-enriched MoS₂ for kinetics-enhanced potassium storage

Guangshen Jiang¹, Xiaosa Xu¹, Haojie Han¹, Changzhen Qu¹, Hlib Repich¹, Fei Xu^{1,2,*}, and Hongqiang Wang^{1,*}

¹ Northwestern Polytechnical University, China

² Technische Universität Dresden, Germany



Edge-enriched MoS₂

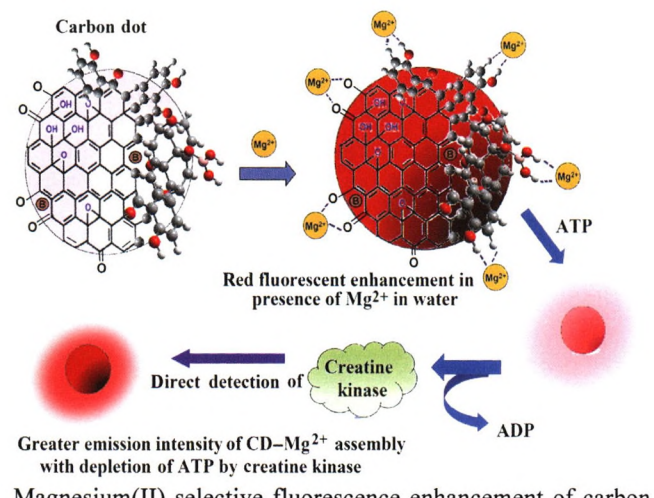
Edge-enriched MoS₂ (EE-MoS₂) was designed with bicontinuous mesoscale skeletons and mesopores, rendering its intrinsic layer spacing more accessible for K⁺ and accelerating conversion kinetics, thus realizing enhanced capacity and high rate capability.

2763–2769

Amplified fluorescence of Mg²⁺ selective red-light emitting carbon dot in water and direct evaluation of creatine kinase activity

Saptarshi Mandal, Jagannath Pal, Ranga Subramanian, and Prolay Das*

Indian Institute of Technology Patna, India



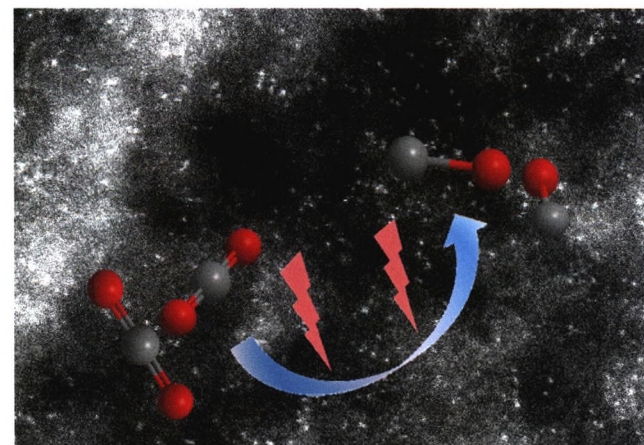
2770–2776

Advanced Ni-N_x-C single-site catalysts for CO₂ electroreduction to CO based on hierarchical carbon nanocages and S-doping

Yiqun Chen¹, Yuejian Yao¹, Yujian Xia², Kun Mao¹, Gongao Tang¹, Qiang Wu^{1,*}, Lijun Yang^{1,*}, Xizhang Wang¹, Xuhui Sun², and Zheng Hu^{1,*}

¹ Nanjing University, China

² Soochow University, China



Ni-N_x-C single-site catalyst based on the unique hierarchical carbon nanocages exhibits a high plateau of Faradaic efficiency for CO₂ electroreduction to CO in a wide range of -0.6 to -1.0 V. S-doping further enhances the CO partial current by 68% and the Faradaic efficiency to 95% at -0.8 V.

2777–2783

Regulating surface state of WO_3 nanosheets by gamma irradiation for suppressing hydrogen evolution reaction in electrochemical N_2 fixation

Yanqi Du, Cheng Jiang, Li Song, Bin Gao, Hao Gong, Wei Xia, Lei Sheng, Tao Wang*, and Jianping He*

Nanjing University of Aeronautics and Astronautics, China

2784–2790

The enhanced protective effects of salvianic acid A: A functionalized nanoparticles against ischemic stroke through increasing the permeability of the blood-brain barrier

Yaru Li^{1,2}, Xiaojie Zhang¹, Zhifeng Qi^{3,*}, Xueling Guo^{1,2}, Xiaopeng Liu⁴, Wenjuan Shi³, Yang Liu^{1,2,*}, and Libo Du^{1,2,*}

¹ Institute of Chemistry, Chinese Academy of Sciences, China

² Graduate School, University of Chinese Academy of Sciences, China

³ Xuanwu Hospital of Capital Medical University, China

⁴ The Second Hospital of Hebei Medical University, China

2791–2802

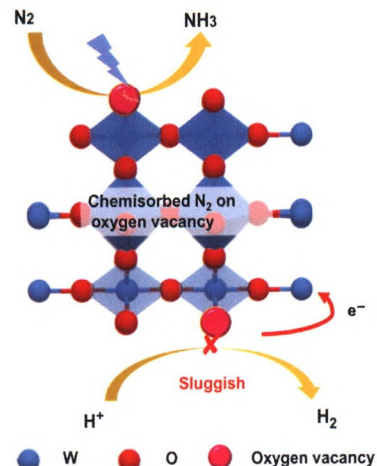
Construction of self-sensitized LiErF_4 : 0.5% Tm^{3+} @ LiYF_4 upconversion nanoprobe for trace water sensing

Ling Zhang¹, Xiaodan Li¹, Wang Wang², Xu Zhao¹, Xu Yan¹, Chenguang Wang¹, Haoqiang Bao¹, Yang Lu¹, Xianggui Kong², Fengmin Liu¹, Xiaomin Liu^{1,*}, and Geyu Lu^{1,*}

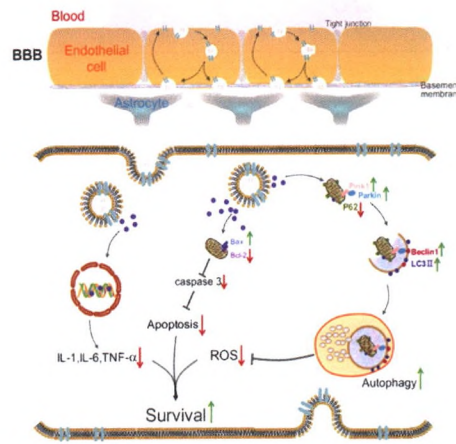
¹ Jilin University, China

² Changchun Institute of Optics, Fine Mechanics and Physics, Chinese Academy of Science, China

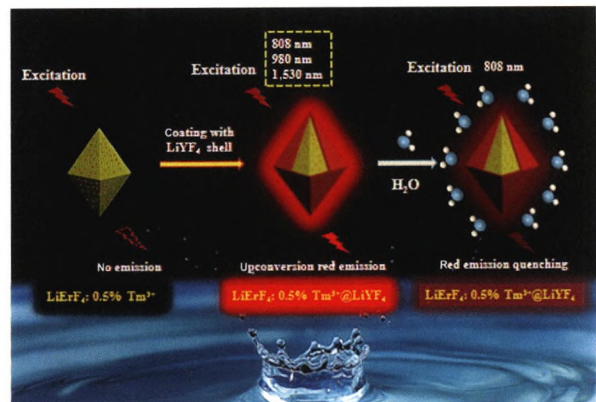
2803–2811



The WO_3 nanosheets with oxygen vacancy were designed for nitrogen reduction reaction (NRR) and tuned electroinc state to suppress hydrogen evolution reaction (HER).



A new type of nanoparticle linked with salvianic acid A (SA) and modified with a targeting peptide, COG1410, that targets the lipoprotein receptors (LPR) on the surface of vascular endothelial cells is fabricated. The potential mechanism of action of the T-SA-NPs in damaged neurons as a result of ischemic stroke is proposed. The internalization of the T-SA-NPs allows the released SA to protect the cells from oxidative stress damage that is induced by ischemic stroke.



We have achieved the strong red upconversion emission based on LiErF_4 system, i.e., LiErF_4 @ LiYF_4 and its relevant derivative LiErF_4 : 0.5% Tm^{3+} @ LiYF_4 , which exhibit strong monochromatic red emission under multiband near-infrared (NIR) excitation (e.g., ~808, ~980 and ~1,530 nm). The Er^{3+} ions enriched nature makes LiErF_4 : 0.5% Tm^{3+} @ LiYF_4 nanoparticles very sensitive for trace water sensing with detection limit of 30 ppm in acetonitrile, 50 ppm in dimethyl sulfoxide (DMSO), and 58 ppm in N,N-dimethylformamide (DMF) under safe excitation of 808 nm.

Plasmonic coupling-enhanced *in situ* photothermal nano-reactor with shape selective catalysis for C–C coupling reaction

Zhenxing Li^{1,*}, Yixuan Gong¹, Xin Zhang¹, Yangyang Wen¹, Jiasai Yao¹, Mingliang Hu¹, Miao He¹, Jiahao Liu¹, Rui Li¹, Fuqiang Wang², and Chuanxin Zhang^{2,*}

¹ China University of Petroleum (Beijing), China

² Harbin Institute of Technology at Weihai, China

2812–2818

A general bottom-up synthesis of CuO-based trimetallic oxide mesocrystal superstructures for efficient catalytic production of trichlorosilane

Hezhi Liu^{1,3}, Yongjun Ji^{2,1,*}, Jing Li¹, Yu Zhang¹, Xueguang Wang³, Haijun Yu⁴, Dingsheng Wang⁵, Ziyi Zhong^{6,7}, Lin Gu⁸, Guangwen Xu⁹, Yadong Li⁵, and Fabing Su^{1,9,10,*}

¹ Institute of Process Engineering, Chinese Academy of Sciences, China

² Beijing Technology and Business University, China

³ Shanghai University, China

⁴ Beijing University of Technology, China

⁵ Tsinghua University, China

⁶ Guangdong Technion–Israel Institute of Technology (GTIIT), China

⁷ Technion–Israel Institute of Technology (IIT), Israel

⁸ Institute of Physics, Chinese Academy of Sciences, China

⁹ Shenyang University of Chemical Technology, China

¹⁰ Zhongke Langfang Institute of Process Engineering, China

2819–2827

Atomically precise metal-chalcogenide semiconductor molecular nanoclusters with high dispersibility: Designed synthesis and intracluster photocarrier dynamics

Jiaxu Zhang¹, Chaochao Qin², Yeshuang Zhong³, Xiang Wang¹, Wei Wang^{1,3}, Dandan Hu¹, Xiaoshuang Liu¹, Chaozhuang Xue¹, Rui Zhou¹, Lei Shen⁴, Yinglin Song¹, Dingguo Xu³, Zhien Lin³, Jun Guo¹, Haifeng Su⁴, Dong-Sheng Li⁵, and Tao Wu^{1,*}

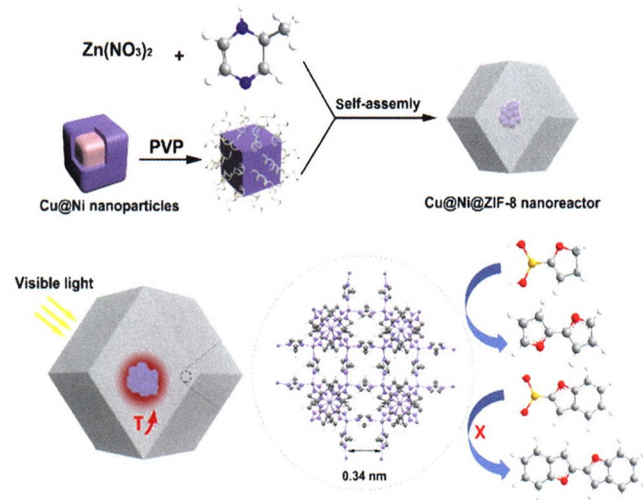
¹ Soochow University, China

² Henan Normal University, China

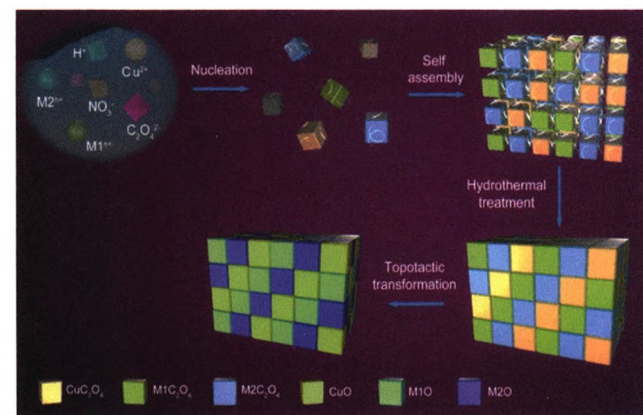
³ Sichuan University, China

⁴ Xiamen University, China

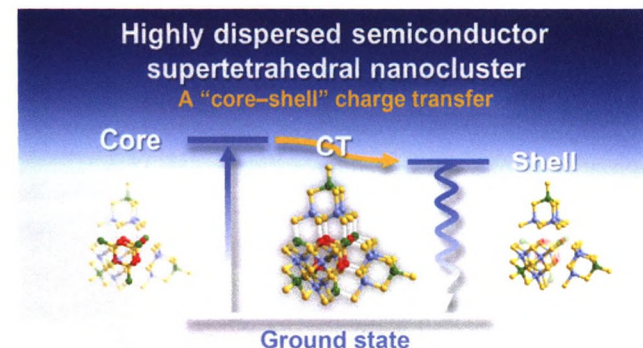
⁵ China Three Gorges University, China



A multifunctional nanoreactor for C–C coupling reaction was successfully designed via encapsulating the core-shell Cu@Ni nanocubes into ZIF-8 (Cu@Ni@ZIF-8).



A general bottom-up synthesis of CuO-based trimetallic oxide mesocrystals (denoted as CuO-M1O_x-M2O_y, where M1 and M2 = Zn, In, Fe, Ni, Mn, and Co) is reported using a simple precipitation method followed by a hydrothermal treatment and a topotactic transformation via calcination.



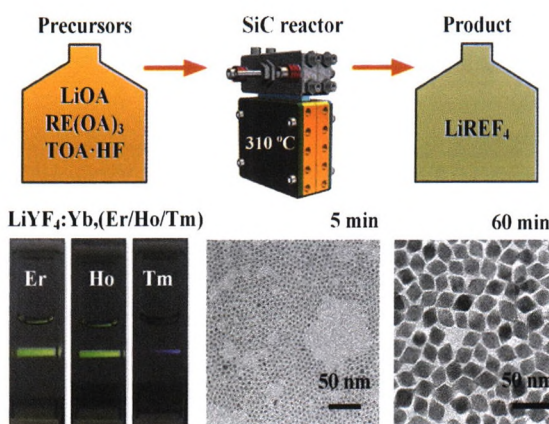
A unique “core–shell” charge transfer relaxation dynamics directed by composition variation was observed in a group of atomically precise semiconductor nanoclusters with targeted high dispersibility in solution.

2828–2836

Efficient synthesis of lithium rare-earth tetrafluoride nanocrystals via a continuous flow method

Jinsong Sui, Junyu Yan, Kai Wang*, and Guangsheng Luo

Tsinghua University, China



A continuous method for synthesizing LiREF_4 nanocrystals was developed with the assistance of a new precursor solution and a silicon carbide (SiC) reactor. The new precursor solution employed trioctylamine (TOA) as the solvent, which prevented the generation of unnecessary solid components, and the space-time yield of the continuous method is about 15 times of that traditional batch reactions.

2837–2846

New approach for time-resolved and dynamic investigations on nanoparticles agglomeration

Neda Iranpour Anaraki^{1,2}, Amin Sadeghpour¹, Kamran Iranshahi^{1,3}, Claudio Toncelli¹, Urszula Cendrowska⁴, Francesco Stellacci⁴, Alex Dommann^{1,5}, Peter Wick², and Antonia Neels^{1,2,*}

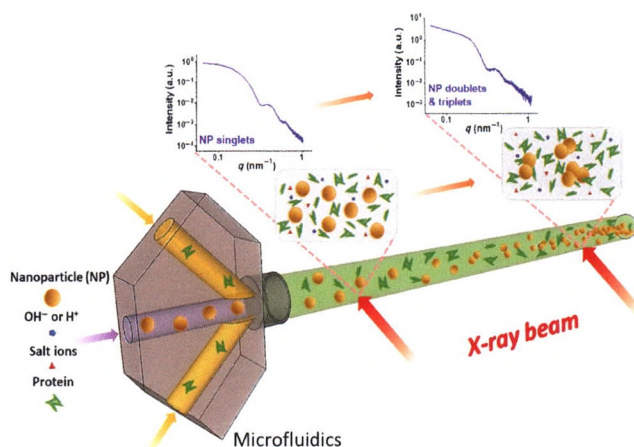
¹ Swiss Federal Laboratories for Materials Science and Technology, Switzerland

² University of Fribourg, Switzerland

³ Swiss Federal Institute of Technology, Switzerland

⁴ EPFL, Switzerland,

⁵ University of Bern, Switzerland



An advanced label-free method based on small-angle X-ray scattering (SAXS) and microfluidic for *in situ* measurements of dynamic processes, namely nanoparticles agglomeration in biological media is reported.

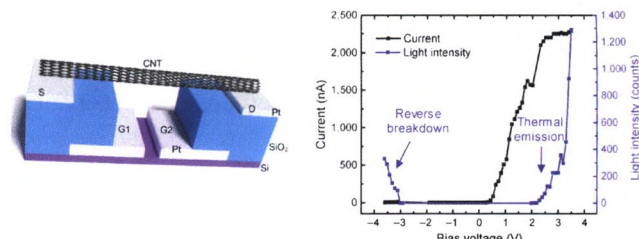
2847–2856

Broadband electroluminescence from reverse breakdown in individual suspended carbon nanotube pn-junctions

Bo Wang¹, Sisi Yang¹, Yu Wang¹, Younghhee Kim², Ragib Ahsan¹, Rehan Kapadia¹, Stephen K. Doorn², Han Htoon², and Stephen B. Cronin^{1,*}

¹ University of Southern California, Los Angeles, USA

² Los Alamos National Laboratory, USA



We report broadband electroluminescence via highly efficient light emission through an avalanche breakdown process from individual suspended carbon nanotube (CNT) dual-gate field effect transistor (FET) devices. The corresponding spectra obtained via thermal emission are considerably narrower than those obtained under reverse breakdown.

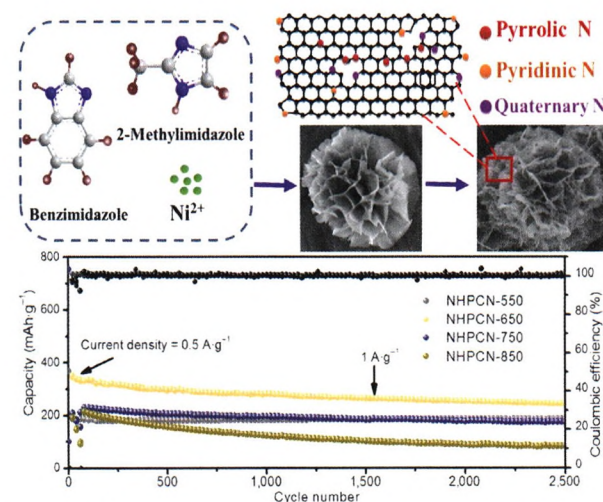
2857–2861

High N-doped hierarchical porous carbon networks with expanded interlayers for efficient sodium storage

Dongqin Su¹, Man Huang¹, Junhao Zhang^{1,*}, Xingmei Guo¹, Jiale Chen¹, Yanchun Xue¹, Aihua Yuan^{1,*}, and Qinghong Kong²

¹ Jiangsu University of Science and Technology, China

² Jiangsu University, China



A novel self-template strategy is designed to synthesize uniform flowerlike N-doped hierarchical porous carbon networks (NHPCN) with high content of N (15.31 at.%), expanded interlayer spacing, ultrathin two-dimensional nano-sized subunits, and three-dimensional porous network structure, delivering outstanding sodium storage performances.

2862–2868

Neglected interstitial space in malaria recurrence and treatment

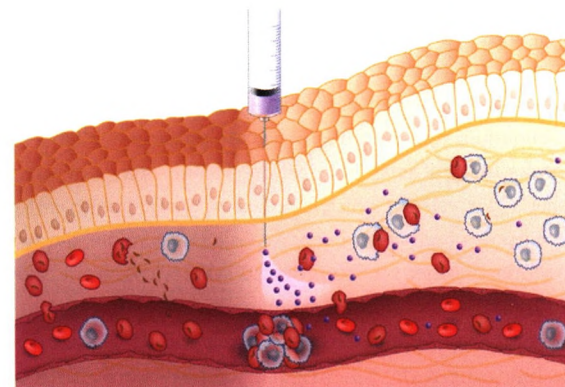
Qiang Zhang^{1,2}, Zhuo Ao^{1,2,*}, Nan Hu^{1,3}, Yuting Zhu¹, Fulong Liao^{1,4}, and Dong Han^{1,2,*}

¹ National Center for Nanoscience and Technology, China

² University of Chinese Academy of Sciences, China

³ Chengde Medical University, China

⁴ China Academy of Chinese Medical Sciences, China



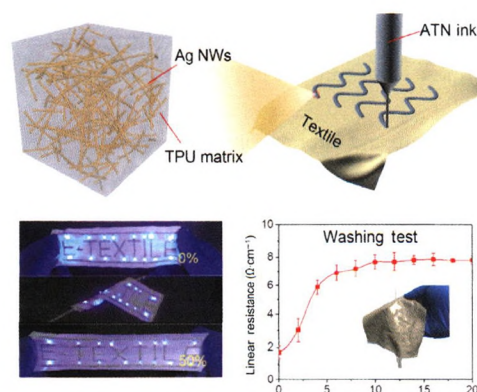
The interstitial space plays an important role that cannot be ignored in the recurrence and treatment of malaria, and may provide a potential way to prevent and treat infectious diseases.

2869–2878

Printable elastic silver nanowire-based conductor for washable electronic textiles

Hong-Wu Zhu, Huai-Ling Gao, Hao-Yu Zhao, Jin Ge, Bi-Cheng Hu, Jin Huang, and Shu-Hong Yu*

University of Science and Technology of China, China



Printable elastic conductor with conductivity of $3,668 \text{ S} \cdot \text{cm}^{-1}$ was developed for electronic textiles (e-textiles). One-step printing of ink could fabricate robust e-textiles, which could endure repeated stretching, folding, and machine washing.

2879–2884

Erratum to: Cobalt phosphide nanoarrays with crystalline-amorphous hybrid phase for hydrogen production in universal-pH (<https://doi.org/10.1007/s12274-020-2881-y>)

2885

ISSN 1998-0124

CN 11-5974/O4

Nano Research

Volume 13 · Number 10 · October 2020

(Monthly, started in 2008)



纳米研究（英文版）（月刊，2008年创刊）第13卷 第10期 2020年10月出版

Editors-in-Chief Yadong Li, Shoushan Fan

Sponsored by Tsinghua University & Chinese Chemical Society

Edited by Nano Research Editorial Office

Published by Tsinghua University Press

Address Xueyan Building,

Tsinghua University,

Beijing 100084, China

Website www.theNanoResearch.com & www.springer.com/journal/12274

Online Manuscript Submission, Review and Tracking System www.editorialmanager.com/nare

主管单位

中华人民共和国教育部

清华大学

中国化学会

主办单位

《纳米研究》编辑部

清华大学出版社有限公司

出版发行

北京地大彩印有限公司

印刷单位

ISSN 1998-0124

